

A New Approach to the Geometry of TOA Location

James J. Caffery, Jr.
University of Cincinnati
Department of ECECS
PO Box 210030
Cincinnati, OH 45221-0030
jcaffery@ececs.uc.edu

Abstract

Positioning a transmitter via measured times of arrival (TOAs), or range measurements, is a familiar technique that has received much attention in the literature. In the traditional geometric interpretation, TOAs generate circles whose intersections provide the estimate of the transmitter. In this paper, a new geometrical interpretation is presented in which straight lines of position (LOPs), rather than the circular LOPs, are used to determine the position of the transmitter. The straight LOPs come from a simple observation regarding the geometry of the system and are not obtained from linearization. Two methods using the straight LOPs are given and their performance is analyzed and compared to methods which employ linearization.

1. Introduction

The problem of positioning a mobile transmitter based on measurements of one or more parameters from a transmitted signal has been of interest for some time. Common parameters that are measured to determine a location fix are time parameters, namely, time of arrival (TOA) and time difference of arrival (TDOA). These two methods are also known as ranging or range-differencing since the time measurements are directly related to ranges (or distances) by the propagation speed of the medium through which the signal travels. For free space, the propagation speed is $c = 3 \times 10^8$ m/s.

Interest in wireless location has been bolstered by the FCC requirements that cellular, PCS, and SMR licensees provide location of mobile stations (MS) for Emergency-911 (E-911) services [2]. While much attention is being given to developing handsets with location technology built into them (e.g., GPS), wireless providers must also provide location services to users with current handsets which have no location functionality. Recently, several papers have

been published giving attention to methods of location in time-division multiple access (TDMA) systems, especially GSM. Because TDMA systems require a method for maintaining time-slot synchronization of the MS transmissions at the receiving base station (BS), the TOA method is one of the possibilities on which to base a location system. The synchronization method known as timing advance (TA) has been discussed in several papers regarding location in GSM [3, 7, 5].

Two approaches can be found in the literature for producing a location estimate from parameter measurements, such as TOA and TDOA: geometrical and statistical. The first is based on the inherent geometrical relationship between the sensor locations and the TOA or TDOA measurements. For TOA, the method of interest in this paper, each range measurement made at a sensor produces a circle centered at that sensor on which the transmitter must lie. Using the circles produced by range measurements at other sensors, the position of the transmitter can be found at the intersection of circles in two-dimensions or spheres in three dimensions. Due to the nonlinearity of the circular lines of position (LOPs), at least one more sensor is needed than the number of dimensions in which the transmitter is to be located. For simplicity, the focus of the remainder of this paper will be on the two dimensional case. The traditional geometrical approach for computing the position of the transmitter is to solve for the intersection of the circular lines of position. This can be a cumbersome task and often does not take into account more than the minimum number of sensors required to make a position fix in two dimensions. Also, when errors are introduced into the measurements, the LOPs do not intersect at a point. This has led to more statistically justifiable methods, such as least squares (LS) algorithms [4, 8, 9].

When approaching location estimation through the geometric point of view, solving this set of equations is a cumbersome task which can be made simpler through a different interpretation of the location geometry. It was shown

previously that the LOPs for a TDOA system need not be hyperbolic, and an alternative geometry which placed the MS's position at the intersection of linear LOPs was derived [6]. In this paper, we show that the LOPs for TOA location also need not be circles, but can be represented in a new geometry as linear LOPs. This has the advantage of simpler computation of location. It also allows the straightforward application of linear statistical location techniques, rather than previous methods which linearize the system or apply nonlinear methods. The new approach to the geometry can aid location systems in TDMA cellular networks, for instance, by allowing them to employ the more simple linear LOPs into their location algorithms.

This paper is organized as follows. Section 2 presents an alternative to the traditional view of the geometry of a TOA location system. Based on this view, Section 3 develops two simple algorithms for location. Results of simulation and analysis are presented in Section 4, followed by conclusions in Section 5.

2 New Geometrical Formulation

As indicated above, the TOA location method measures the range between each sensor and the transmitter which is to be located. This range between the i^{th} sensor and the source can be expressed as

$$D_i = \|\mathbf{x}_i - \mathbf{x}_s\| \quad (1)$$

$$= \sqrt{(x_i - x_s)^2 + (y_i - y_s)^2} \quad (2)$$

where \mathbf{x}_i is the position of the i^{th} sensor, \mathbf{x}_s is the position of the source transmitter, and $\|\mathbf{x}\|$ denotes the norm of the vector \mathbf{x} . The relationship between the ranges for three sensors, their location, and the position of the source are shown in Fig. 1 in two dimensions where the circular LOPs are shown with solid lines.

A new approach to TOA location is based on observations of Fig. 1 [1]. As can be seen from the figure, each circular LOP intersects with another circular LOP at two points. This is the reason that three sensors must be used for location in two dimensions, i.e., to resolve the ambiguity of position. These two points can be used to generate another LOP that is linear and passes through those two points. Since there are three circles, we can use six points to generate three lines (3 of the points are redundant, giving 4 unique points). In Fig. 1, only two lines (dashed) are shown and it can be easily seen where the third line would lie. As indicated in the figure, the new linear LOPs also intersect at the location of the transmitter.

To determine the equations for the new linear LOPs, we must start with the original circular LOP equations, given in equation (2), for $i = 1, 2, 3$. Consider the sensors at \mathbf{x}_1 and \mathbf{x}_2 . The line which passes through the intersection of

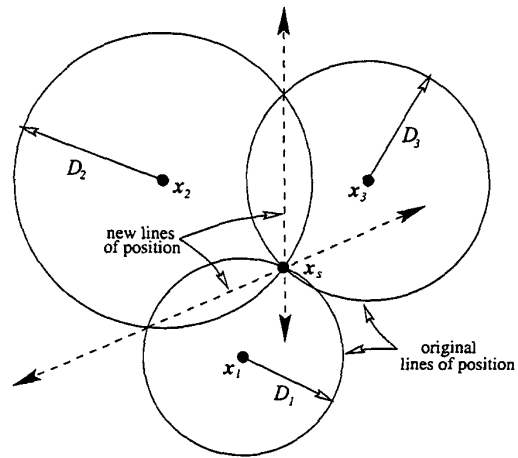


Figure 1. Geometry of TOA-based location showing circular LOPs and linear LOPs.

the two circular LOPs for those two sensors can be found by squaring and differencing the ranges in (2) for $i = 1, 2$, which results in

$$(x_2 - x_1)x_s + (y_2 - y_1)y_s = \frac{1}{2} (\|\mathbf{x}_2\|^2 - \|\mathbf{x}_1\|^2 + D_1^2 - D_2^2) \quad (3)$$

for the new LOP. Following the same procedure for $i = 2, 3$ yields the line

$$(x_3 - x_2)x_s + (y_3 - y_2)y_s = \frac{1}{2} (\|\mathbf{x}_3\|^2 - \|\mathbf{x}_2\|^2 + D_2^2 - D_3^2) \quad (4)$$

for sensors at \mathbf{x}_2 and \mathbf{x}_3 .

A similar linear LOP can be generated for sensors 1 and 3; however, it can be easily shown that the third LOP from this set of three sensors is not independent from the other two LOPs. The reason is that the third line can be generated by simply adding the two equations above, which eliminates all terms involving sensor 2, leaving an equation identical to (3), but with \mathbf{x}_2 and D_2 replaced with \mathbf{x}_3 and D_3 , respectively. It is easy to show that the line generated by adding the two equations above is the same that would be produced by the squaring and differencing procedure above. Thus, while it is possible to obtain three linear LOPs, only two are independent, and as it turns out, the third will always intersect the other two LOPs at the same point that they intersect each other, even if there are errors in the measured TOAs. Based on this fact, a location algorithm based on the intersecting linear LOPs only requires two of the possible three LOPs that could be generated.

Given the two linear LOPs above, the location of the source can be obtained by solving (3) and (4) for y_s , equat-

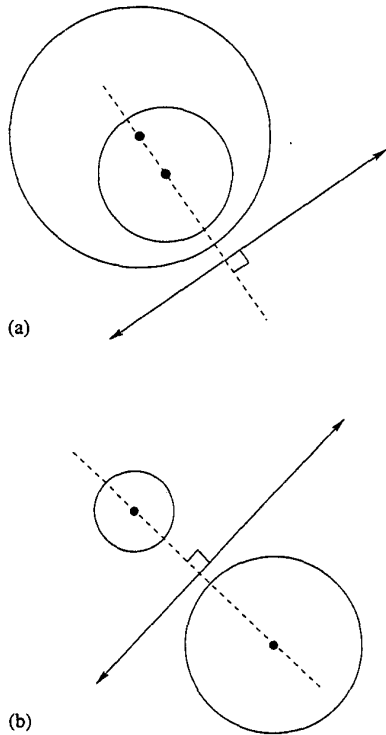


Figure 2. The relation of lines to the circles when there is no intersection of the circles.

ing those results, and solving for x_s which produces

$$x_s = \frac{(y_2 - y_1) C_3 - (y_3 - y_2) C_1}{[(x_3 - x_2)(y_2 - y_1) - (x_2 - x_1)(y_3 - y_2)]} \quad (5)$$

where

$$C_1 = \frac{1}{2} (\|x_2\|^2 - \|x_1\|^2 + D_1^2 - D_2^2) \quad (6)$$

$$C_3 = \frac{1}{2} (\|x_3\|^2 - \|x_2\|^2 + D_2^2 - D_3^2) \quad (7)$$

Substituting this result into either (3) or (4) and solving for y_s gives

$$y_s = \frac{(x_2 - x_1) C_3 - (x_3 - x_2) C_1}{[(y_3 - y_2)(x_2 - x_1) - (y_2 - y_1)(x_3 - x_2)]} \quad (8)$$

One consideration that must be accounted for is the possibility that two of the circular LOPs will not intersect another due to measurement errors in the TOAs. Two possibilities in this regard are illustrated in Fig. 2. In both cases, it is still possible to generate linear LOPs from the circular LOPs using the equations in (3) or (4). Even though there

is not intersection of the circles, a straight line is still produced. Note that the lines in Fig. 1 are perpendicular to the baseline connecting the two sensors whose circular LOPs intersect. As a result, it is also parallel to the tangents of the two circular LOPs at the point where the baseline intersects the circles. In keeping with this, the linear LOPs that are produced from the non-intersecting circular LOPs are also perpendicular to the baseline connecting the two sensors and hence parallel to tangents of the two circles at the points where the baseline intersects the circles. As mentioned previously, even when the TOAs contain measurement errors and two or more circular LOPs do not intersect, all three of the LOPs that can be generated intersect at the *same* point and the third LOP can be generated from the other two. Two final notes are of interest. First, three sensors are still the minimum required to locate a source in two dimensions using this approach. Secondly, the equations require that no baselines connecting the sensors be horizontal or vertical. If this is the case, a simple rotation of the coordinate system can be used and rotated back after a solution is obtained.

3. Algorithms

The previous section developed the new “location geometry” for locating a sensor in two dimensions with three sensors. In practice, we would like to use the method when there are more than the minimum number (i.e., greater than three sensors in two dimensions) and when there are measurement errors in the TOAs. As discussed in the introduction, two approaches to algorithm development can be taken: determining location by solving for the intersection of LOPs or statistical approaches. In the following, both an intersection (geometry based) solution and a least squares (LS) solution are discussed.

3.1. Intersection of LOPs

A simple approach to location using the linear LOPs was developed in Section 2 for three sensors. Calculating the intersection of the linear LOPs produced the location estimate. For more than three receivers in the presence of ranging error, many more linear LOPs can be produced which do not all intersect at the same point, as they did with three sensors. For instance, with four sensors a total of 12 linear LOPs can be produced from the intersections of the four circles. For each set of three circles (four total) three linear LOPs can be produced all of which intersect at the same point. Hence, at least 4 lines are redundant (for intersection purposes) and can be ignored. Of the remaining eight, five more can be ignored since the remaining three (or combinations of them) can produce the other five. Thus, for four

sensors only three lines are necessary to compute three intersections.

To understand where these numbers come from, consider sensors $i = 1, 2, 3, 4$. Four sets of three sensors can be obtained as follows: (1,2,3), (1,2,4), (1,3,4) and (2,3,4). Each of these sets can produce three lines, one of which is redundant, and a single point of intersection. When all lines are considered together, the number of intersections is much higher as discussed below. Let (i, j) denote the line produced by the intersection of the circular LOPs of sensors i and j . Then, (1,2)+(1,3) yields (2,3), (1,2)+(1,4) yields (2,4), (1,3)+(1,4) yields (3,4), and (2,3)+(2,4) yields (3,4). We will refer to lines that can be formed from a base set of lines as *redundant*. Of the eight remaining lines, (1,2), (1,3), and (1,4) each occur twice, which eliminates three more. Also, (2,4) and (2,3) are redundant in that they can be produced by (1,2)+(1,4) and (1,2)+(1,3), respectively. The remaining three lines, (1,2), (1,3), and (1,4), are non-redundant and can produce all of the original 12 lines. These three lines can be used to compute either the original four points of intersection of each of the original four sets or just the three unique points of intersection of those three lines. From those intersections, the location estimate can be computed by either finding the mean of those points, or the centroid of the triangle formed by those three points.

This approach can be generalized for N total sensors where non-redundant $N - 1$ lines can be used to produce all of the original $C(N, 3) \times 3$ lines from the intersections of the N circles, where $C(n, m) = n!/m!(n - m)!$. The $N - 1$ linear LOPs could be described, for instance, by the lines (1, 2), (1, 3), ..., (1, $N - 1$) and (1, N). These $N - 1$ linear LOPs could then be used to compute the intersection points of the $C(N, 3)$ original sets of lines (formed by combining three sensors into a set). Alternatively, all of the intersections of the $N - 1$ non-redundant lines could be used to compute $(N - 1)(N - 2)/2$ intersection points of those lines. As in the example above, the location of the source could be found from the mean of the intersection points or the centroid of a polygon formed by those points.

Obviously, the more sensors that are used, the more complicated can be the solution using intersecting LOPs.

3.2. Least Squares (LS)

An alternative approach to the solution of geometric equations is to compute the position of the source using a LS approach when there are $N > 3$ sensors making TOA measurements. Each of the $N - 1$ non-redundant lines is of the form (see equation (3)):

$$a_{i,1}x_s + a_{i,2}y_s = a_i^T x_s = b_i \quad (9)$$

for the i^{th} line, where $a_i = [a_{i,1} \ a_{i,2}]^T$ and $x_s = [x_s \ y_s]^T$. The system of equations describing all of the

lines can be written in matrix form as

$$A x_s = b \quad (10)$$

where $A^T = [a_1 \ a_2 \ \dots \ a_G]$ and $b = [b_1 \ b_2 \ \dots \ b_G]^T$, and G is the number of lines used. Due to measurement errors which are contained in the vector b , a LS solution is used, resulting in the LS estimate for x_s as

$$\hat{x}_s = (A^T A)^{-1} A^T b \quad (11)$$

The minimum number of linear LOPs used for the LS solution is $G = N - 1$, the number of non-redundant lines. However, since the LS solution finds the estimate that is closest to the LOPs, we can use more than the minimum number. The additional lines can be considered since in the LS solution, we are not interested in computing the intersections of lines. The maximum number of lines that can be used in the LS algorithm is $3C(N, 3)/(N - 2)$. This number takes into account the fact that the lines generated from all possible combinations of three sensors ($C(N, 3)$) occur multiple times. Hence, the size of the matrix A and vector b are limited by $N - 1 \leq G \leq 3C(N, 3)/(N - 2)$. This algorithm is obviously much less difficult than the geometric one since there is no need to compute intersections of many lines.

4. Performance

Various simulations were performed to assess the performance of the algorithms discussed in the previous section. In the simulations, the sensors were located at $x_1 = [0 \ 0]^T$, $x_2 = [2000 \ 2500]^T$, $x_3 = [5000 \ 2000]^T$ and $x_4 = [3000 \ 1500]^T$. The source was randomly placed around the sensors. The TOA measurements were each corrupted by zero-mean white Gaussian noise (WGN) in some simulations, and by a non-zero mean WGN in others to represent measurement bias as might occur in non-line-of-sight (NLOS) transmissions. The algorithms were also compared to LS algorithms based on Taylor series linearization (TS-LS) [4, 8].

In each of the figures that follow, results for three and four BSs (or sensors) are provided. For the three sensor case, the intersection of two linear LOPs is used for the "line intersection" method, whereas in the four sensor case, the mean of the three points of intersection from the three non-redundant LOPs was used as the estimate. For the LS solutions in the four sensor case, the number of lines used in the algorithm varies from the minimum ($G = 3$) to the maximum ($G = 6$). The TS-LS solutions are based on the Taylor series LS algorithms referenced above. Furthermore, the figures are divided depending whether the source was located within the perimeter of the sensors or outside of it.

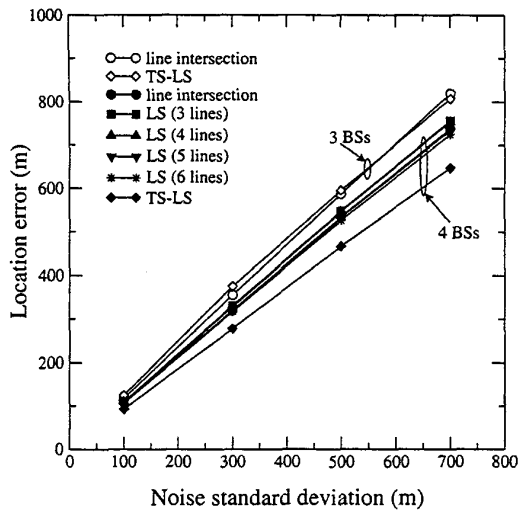


Figure 3. The location error versus the standard deviation of the measurement noise for various location algorithms with 3 and 4 sensors. The error is computed for locations *inside* the perimeter of sensors.

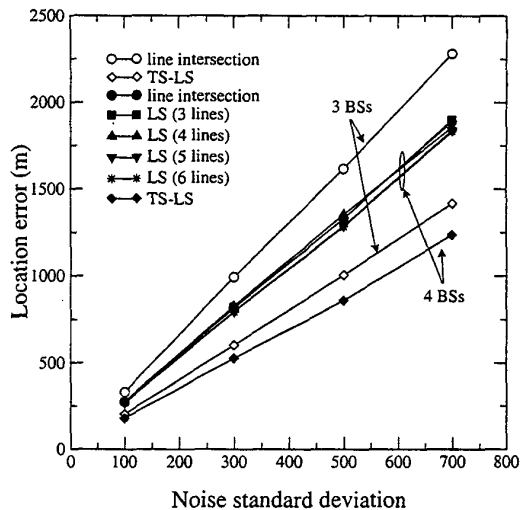


Figure 4. The location error versus the standard deviation of the measurement noise for various location algorithms with 3 and 4 sensors. The error is computed for locations *outside* the perimeter of sensors.

We will find that this makes a difference in performance due to the algorithms dependence on the geometry of the sensor positions.

Fig. 3 shows the mean location error for the several algorithms for various noise standard deviations (no bias) while the source was located inside the perimeter of the sensors. The figure shows that the performance is decreased as the standard deviation of the noise is increased, which is expected. The linear intersection method for three sensors is shown to perform nearly identically to the TS-LS algorithm. For four sensors, all of the linear LS methods perform closely regardless of the number of lines, G , used. Also, they perform slightly worse than the four sensor TS-LS algorithm, with the discrepancy increasing with increasing noise standard deviation.

Fig. 4 shows a similar plot but where the source was restricted to outside the perimeter area of the sensors. In this case, the algorithms based on the new geometry perform much worse than the TS-LS methods. In fact, the three sensor TS-LS algorithm outperforms the four sensor linear LS methods of the previous section. These results indicate the importance of geometry on the performance of an algorithm.

Fig. 5 shows the effect that a measurement bias (non-zero mean WGN) can have on performance. The standard deviation of the bias was 100 m, so that the bias dominated

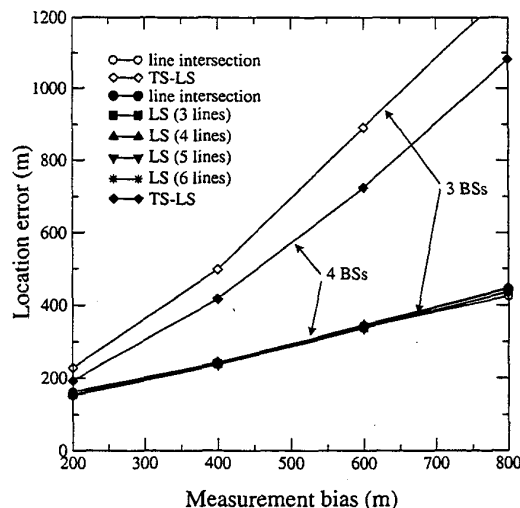


Figure 5. The location error versus the measurement bias for various location algorithms with 3 and 4 sensors. The error is computed for locations *inside* of the perimeter of sensors.

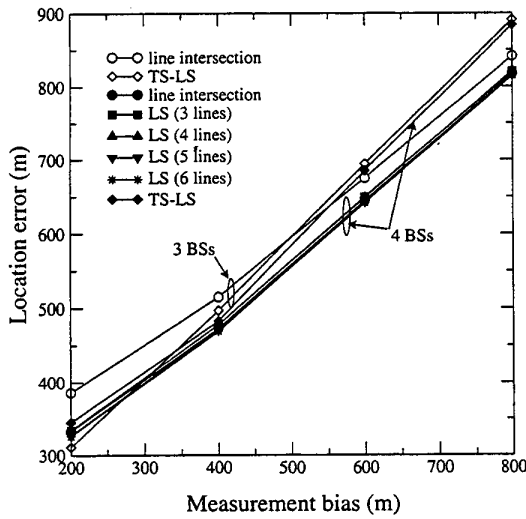


Figure 6. The location error versus the measurement bias for various location algorithms with 3 and 4 sensors. The error is computed for locations *outside* of the perimeter of sensors.

the performance. For positions inside the perimeter of the sensors, it is found that all of the algorithms based on the new geometry drastically outperformed the TS-LS methods. In fact, the simple three sensor line intersection method greatly outperformed the four sensor TS-LS algorithm.

Finally, Fig. 6 show similar results for positions outside the perimeter of sensors. The four sensor linear LS algorithms of this paper outperformed the other algorithms, particularly for high biases. At high biases, the TS-LS algorithms perform equally poorly compared to the linear LS for all values of G . The line intersection method for four sensors performs identically to the linear LS algorithms, while for three sensors, it performs worse, but not as bad as the TS-LS algorithms for large bias values.

To illustrate graphically the difference in dependence that the linear LS approach of this paper and the TS-LS algorithm have on geometry, we generated surface plots of the error for an area encompassing the four sensors. The error surfaces were generated by adding an error of 50 m to the TOA measurement of the first sensor (located at x_1). The TOAs for the other sensors were exact. The surfaces in Figs. 7, 8, and 9. Fig. 7 shows the error surface for the TS-LS algorithms using three sensors. The \times 's on the $x - y$ plane indicate the positions of the sensors. A contour mapping of the surface is also shown on the $x - y$ plane. Fig. 8 shows the surface for the linear LS method using four sensors and three (the minimum) LOPs. It is interesting to

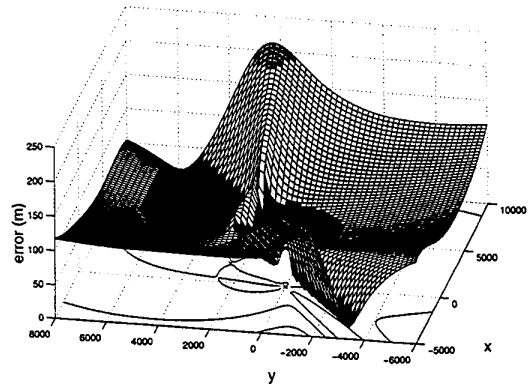


Figure 7. Error surface generated for the TS-LS location algorithm using three sensors. The range measurement for sensor 1 is perturbed by 50 m.

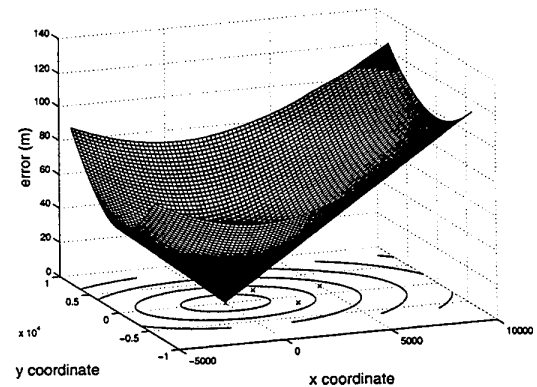


Figure 8. Error surface generated for the straight-line LS location algorithm based on three lines using four sensors. The range measurement for sensor 1 is perturbed by 50 m.

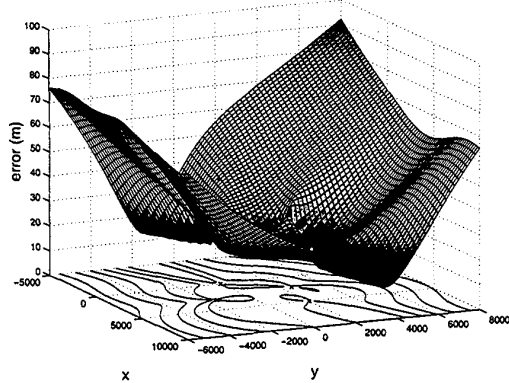


Figure 9. Error surface generated for the TS-LS location algorithm using four sensors. The range measurement for sensor 1 is perturbed by 50 m.

note that the error increases almost linearly as one moves away from the position of sensor 1 (at (0,0)). In the previous figure, the error was minimized near and in between the sensors, but not for the linear LS algorithm whose error surface seems to depend completely on the position of the sensor with the erred TOA measurement. Finally, Fig. 9 shows the error surface for the TS-LS algorithm using four sensors. The geometry shapes the surface much differently than the three sensor case.

5. Conclusions

A new interpretation of the geometry of TOA location has been presented. The approach replaced the circular LOPs, typically associated with ranging, with linear LOPs. Two algorithms were discussed from the new geometry. The geometrical solution found the intersection of the linear LOPs and used the mean of those intersections for a location estimate. A LS solution was based on the linear equations representing the LOPs. Simulations showed that the performance was slightly worse than LS with Taylor series linearization (TS-LS) when the TOA measurements were corrupted by zero-mean WGN both inside and outside the perimeter of the sensors. However, the performance of the linear LS algorithm was significantly better than the TS-LS algorithm when a large bias was present. This may find some significant role in wireless location for E-911 since non-line-of-sight propagation introduces a bias in measurements. Also, the the results near and inside the perimeter of the sensors are more significant for wireless location in cellular systems since the most probably BSs to be used for

location are those that lie closest to the MS.

References

- [1] J. Caffery, Jr. *Wireless Location in CDMA Cellular Radio Systems*. Kluwer Academic Publishers, 1999.
- [2] CC Docket No. 94-102. Revision of the commissions rules to ensure compatibility with enhanced 911 emergency calling systems, RM-8143, July 26 1996.
- [3] C. Drane, M. Macnaughtan, and C. Scott. Positioning GSM Telephones. *IEEE Communications Magazine*, pages 46–59, Apr. 1998.
- [4] W. Foy. Position-location solutions by Taylor-series estimation. *IEEE Trans. on Aerospace and Electronic Systems*, AES-12:187–193, Mar. 1976.
- [5] J. Reed, K. Krizman, B. Woerner, and T. Rappaport. An overview of the challenges and progress in meeting the e-911 requirement for location service. *IEEE Communications Magazine*, 36:30–37, Apr. 1998.
- [6] R. Schmidt. A new approach to geometry of range difference location. *IEEE Trans. on Aerospace and Electronic Systems*, AES-8:821–835, Nov. 1972.
- [7] M. Silventoinen and T. Rantalainen. Mobile station emergency locating in GSM. In *IEEE Int. Conference on Personal Wireless Communications*, pages 232–238, 1996.
- [8] D. Torrieri. Statistical theory of passive location systems. *IEEE Trans. on Aerospace and Electronic Systems*, AES-20:183–197, Mar. 1984.
- [9] G. Turin, W. Jewell, and T. Johnston. Simulation of urban vehicle-monitoring systems. *IEEE Trans. on Vehicular Technology*, VT-21:9–16, Feb. 1972.